

Nanoscale

Accepted Manuscript



This is an *Accepted Manuscript*, which has been through the Royal Society of Chemistry peer review process and has been accepted for publication.

Accepted Manuscripts are published online shortly after acceptance, before technical editing, formatting and proof reading. Using this free service, authors can make their results available to the community, in citable form, before we publish the edited article. We will replace this *Accepted Manuscript* with the edited and formatted *Advance Article* as soon as it is available.

You can find more information about *Accepted Manuscripts* in the [Information for Authors](#).

Please note that technical editing may introduce minor changes to the text and/or graphics, which may alter content. The journal's standard [Terms & Conditions](#) and the [Ethical guidelines](#) still apply. In no event shall the Royal Society of Chemistry be held responsible for any errors or omissions in this *Accepted Manuscript* or any consequences arising from the use of any information it contains.



Nanoscale

COMMUNICATION

Hybrid Van der Waals Heterostructures of Zero-Dimensional and Two-Dimensional Materials

Received 00th January 20xx,
Accepted 00th January 20xx

Zhikun Zheng^{*ab}, Xianghui Zhang^a, Christof Neumann^a, Daniel Emmrich^a, Andreas Winter^c, Henning Vieker^{†a}, Wei Liu^d, Marga Lensen^e, Armin Götzhäuser^a and Andrey Turchanin^{*c}

DOI: 10.1039/x0xx00000x

www.rsc.org/

Van der Waals heterostructures meet other low-dimensional materials. Stacking of about 1 nm thick nanosheets with out-of-plane anchor groups functionalized with fullerenes integrates this zero-dimensional material into layered heterostructures with well-defined chemical composition and without degrading the mechanical properties. The developed modular and highly applicable approach enables the incorporation of other low-dimensional materials, e.g. nanoparticles or nanotubes, into heterostructures significantly extending the possible building blocks.

Molecular assembly of materials with precise control over their chemical composition, thickness and structure is in the focus of physical, chemical and materials science research already for many years.¹⁻⁹ This interest is motivated by engineering materials with controlled functionalities on demand. To this end, various techniques have been developed. Typical examples are Langmuir-Blodgett (LB) technique, layer-by-layer (LbL) assembly, and self-assembled monolayers (SAMs). They have been widely used to assemble zero- and one-dimensional (0D, 1D) materials such as small molecules, nanoparticles, biomolecules, polyelectrolytes and nanotubes/-wires.¹⁻⁸ With the demonstration of free-standing atomically or single-molecularly thick sheets,¹⁰⁻¹² stacking them vertically in a chosen way serves as a new technique to create designed artificial materials, so-called van der Waals (vdW) heterostructures.^{9,13,14} Combination of these 2D sheets including graphene, hexagonal boron nitride or metal chalcogenides have led to mechanically stable heterostructures with a high potential for applications in sensors and flexible electronics.^{9,15} Recent research

efforts have also been focused on the developing of various covalent and non-covalent functionalization approaches to combine 2D sheets with 0D and 1D materials.¹⁶⁻²⁰ However, it remains a major challenge to assemble stable stacks of 0D/1D materials with 2D sheets without degrading the mechanical properties of the pristine sheets. Non-covalent interactions, such as van der Waals interactions and π - π stacking, are not strong enough to stably immobilize 0D/1D materials on 2D sheets. Thus the adhered materials can be easily removed by solvent rinsing or even with time and by environmental moisture.^{16,19,20} On the other hand, strong covalent interactions require a change in the integral structure of 2D sheets, which degrade their initial mechanical properties.

In this work, we present a modular and broadly applicable route to create hybrid vdW heterostructures made of individual ~ 1 nm thick single molecular sheets, Janus nanomembranes (JNMs),^{13,21} which have well-defined anchor groups on their opposite sides, see Figure 1, and other low-dimensional materials. JNMs are generated via electron irradiation of 4'-nitro-1,1'-biphenyl-4-thiol (NBPT) SAMs resulting in their crosslinking via formation of lateral covalent bonds and simultaneous conversion of the terminal nitro groups into amino groups²² and the subsequent release from the original substrates via the poly(methyl methacrylate) (PMMA) assisted transfer process.^{23,24} The upper side of the JNM has amino groups (N-side) and the lower side has sulfur species (S-side), see Figure 1c; both sides can be independently and chemically functionalized.²¹ Using chemical functionalization of JNMs with the desired building blocks on their one or both faces and subsequent stacking, hybrid vdW heterostructures can be assembled. In our proof-of-concept experiments, we utilize 0D carbon – fullerene C₆₀ – as a functional nanomaterial and covalently bind to the amino groups of JNMs; we also demonstrate functionalization of the S-side with Au nanoparticle (NPs), see Figure 1d. We fabricate heterostructure stacks of the C₆₀-JNM hybrid and characterize their structural, chemical and mechanical properties by optical microscopy, helium ion microscopy (HIM), X-ray photoelectron spectroscopy (XPS) and mechanical bulging tests. To make the S-side of JNMs accessible for post-modification under various experimental conditions, a universal flip-over procedure for JNMs was developed.

^a Faculty of Physics, University of Bielefeld, 33615 Bielefeld, Germany.

^b Department of Chemistry and Food Chemistry, TU Dresden, 01069 Dresden, Germany. Email: zhikun.zheng@tu-dresden.de

^c Institute of Physical Chemistry, Friedrich Schiller University Jena, 07743 Jena, Germany. Email: andrey.turchanin@uni-jena.de

^d Physical Chemistry and Center for Advancing Electronics Dresden, TU Dresden, 01069 Dresden, Germany.

^e Institute of Chemistry, Technische Universität Berlin, 10623 Berlin, Germany.

[†] Current address: CNM Technologies, 33602 Bielefeld, Germany.

Electronic Supplementary Information (ESI) available: See

DOI: 10.1039/x0xx00000x.

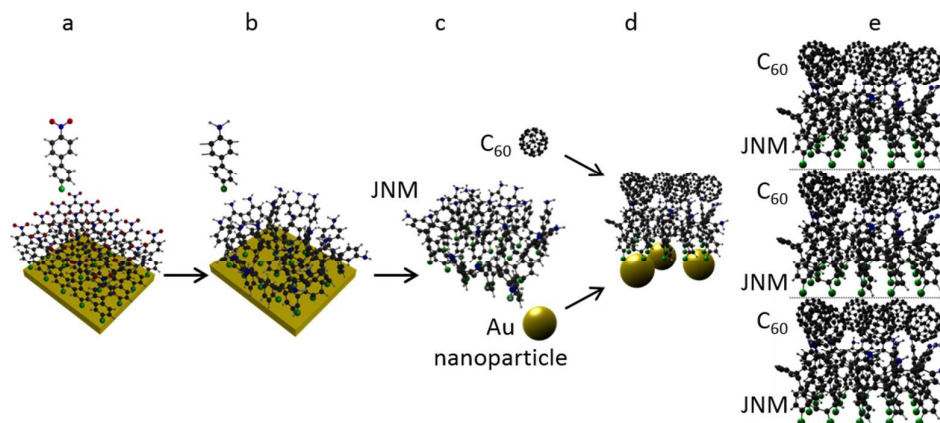


Figure 1. Schematic representation of the heterostructure assembly. a) Formation of a NBPT SAM on a gold substrate. b) Electron irradiation induced crosslinking and reduction of the terminal nitro groups into amino groups. c) Formation of a free-standing JNM with the terminal N- and S-faces. d) Functionalization of the N- and S-faces with C_{60} and AuNP, respectively. e) Assembly of a $(C_{60}\text{-JNM})_n$ (here $n=3$) hybrid heterostructure by mechanical stacking. Color code for atoms: black – carbon, grey – hydrogen, blue – nitrogen, green – sulfur, and red – oxygen.

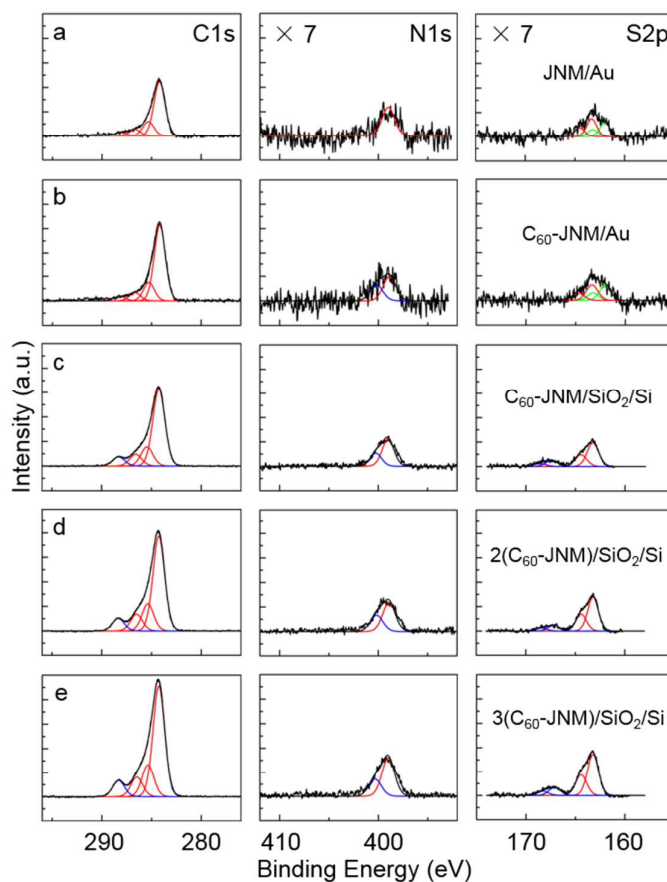


Figure 2. XPS characterization. a) JNM on the original gold substrate. b) $C_{60}\text{-JNM}$ on the original gold substrate. $C_{60}\text{-JNM}$ monolayer/multilayer after transfer onto 285 nm SiO_2/Si (monolayer c), bilayer d) and trilayer e)). Intensities of the S_{2p} and N_{1s} spectra were multiplied by 7.

To assemble C_{60} -JNM heterostructures, we synthesized JNMs on gold substrates (JNM/Au), immobilized C_{60} onto the N-side of the JNMs, and stacked the C_{60} -JNM hybrids on top of each other. The successful immobilization of C_{60} onto JNM/Au was confirmed by XPS. Figure 2a shows the XP spectra of a JNM/Au. The C1s signal consists of several peaks with binding energies (BEs) at 284.2 eV and 285.3 eV, which are due to the aromatic carbon and the C-S/C-N bonds, respectively; and the aromatic shake-up satellites at 287–290 eV.²⁴ The N1s signal at 399.3 eV is characteristic for amino groups. The S2p signal shows the presence of two sulfur species with the S2p_{3/2} BEs at 162.0 and 163.2 eV, which are due to thiulates and sulfides/disulfides formed upon irradiation,²⁵ respectively. The effective thickness of a JNM calculated from the attenuation of the Au4f_{7/2} signal is about 1.1 nm.²⁶ In Figure 2b the XP spectra of a JNM with C_{60} grafted to the amino groups are presented.²⁷ The successful grafting is confirmed by the corresponding changes of the respective XP signals. The total intensity of the C1s signal increases by ~30% and a new N1s peak at ~400.3 eV appears due to the formation of C-N bonds.^{27–29} The intensity ratio between this peak and the total N1s intensity is ~30%, which indicates the percentage of the amino groups on forming chemical bonds with C_{60} . Intensity of the S2p signal decreases showing an increase of the hybrid thickness (see Table S1 for thickness change).

To demonstrate that C_{60} -JNMs can be released from their original substrate and further used for fabrication of the heterostructures, we tested their transfer onto 285 nm SiO₂/Si substrates by the PMMA assisted process.²⁴ These substrates were chosen as they enable the observation of JNMs by optical interference (see Fig. S1a).¹⁴ Figure 2c shows XP spectra of the transferred C_{60} -JNM. The characteristics of the XP signals are similar to those of the pristine C_{60} -JNM/Au. A slight increase of the C1s peak at ~288.3 eV is observed, which is most likely due to the presence of some PMMA residuals after the transfer.³⁰ The S2p_{3/2} signal at 162.0 eV disappears and the intensity of the S2p_{3/2} signal at 163.2 eV increases significantly due to the transformation of thiulates into sulfides/disulfides or into unbound thiols during the transfer process.²¹ A new doublet appears with S2p_{3/2} at 167.2 eV caused by the oxidation of thiulates/sulfide/disulfides to sulfonic group.³¹ Note that the sulfonic group is negatively charged in water, which can be used for the functionalization of the S-side of JNMs by electrostatic interactions.

For the fabrication of cm²-sized patterned C_{60} -JNM heterostructures on 285 nm SiO₂/Si, a simple method was applied. C_{60} -JNM sheets on Au/mica substrates were cut with scissors into rectangular stripes of width ~0.5 cm and then the sheets were transferred onto the Si-wafer by putting them on top of each another in different orientations. This procedure leads to the formation of regions with either no, one, two or three sheets (Figure S1a). Note that the uniform contrast within the areas with varying numbers of C_{60} -JNM sheets reflects their homogeneous thickness.

As only the electron irradiated areas of NBPT SAMs are converted into JNMs and there is no lateral crosslinking between molecules in the non-irradiated areas, it is possible by selective electron irradiation to pattern JNMs, functionalize them with C_{60} and then transfer the patterned C_{60} -JNM onto a new substrate (Figure S1b).

Such a procedure makes it possible to produce the JNM-based hybrids in any shape without additional resist materials either by using electron irradiation through stencil masks, as in this experiment, or by standard electron beam lithography.

The assembled heterostructure stacks were characterized by XPS. We found no significant changes in the shapes of C1s, S2p and N1s signals for the bi-layer and the tri-layer of C_{60} -JNM (Figure 2d and 2e), which indicate that each layer has a similar chemical composition. The obtained effective thickness of the bi-layer and tri-layer stacks is ~3.7 nm and ~5.4 nm, respectively, which confirms further homogeneous contributions of each layer to the total structure. This homogeneity benefits from the high reproducibility by functionalization of mechanically stable JNMs, which is difficult to achieve employing the layer-by-layer growth on conventional SAMs.^{32–34}

To quantitatively characterize the mechanical properties of individual C_{60} -JNMs and their heterostructures, they were studied by mechanical bulge tests. To this end, the sheets were transferred onto a silicon substrate with an array of square shaped orifices. Figure 3a shows a helium ion microscopy (HIM) image of a C_{60} -JNM hybrid. An orifice with the spanned C_{60} -JNM is observed (marked with “freestanding”), which indicates that the hybrid can support its own weight and preserve its mechanical integrity. Apart from the large homogeneous area, some wrinkles or ruptures (Figure 3b–3c) are observed, which are typical for mechanically robust nanosheets.¹⁰ Figure 3d shows a homogeneous freestanding JNM/(C_{60} -JNM)₃ heterostructure spanning over an orifice with dimensions of 40×44 μm². The heterostructure in Figure 3e shows some wrinkles, which increase the imaging contrast and help to identify the freestanding membrane by HIM. Note that only the homogeneous structures as in Figure 3d were employed for bulge tests with an atomic force microscope (AFM). To assure that the interaction between a (C_{60} -JNM)_n and an AFM tip is the same as that for an individual JNM, a JNM was placed on top of the respective heterostructures forming the JNM/(C_{60} -JNM)_n stacks. The testing was performed by adjusting an AFM tip to the nanomembrane center,^{35,36} as schematically shown in Figure 3f. Different N₂ pressure is applied beneath the membrane, and its corresponding deflection is then recorded by AFM. Figure 3g shows a typical pressure-deflection curve for a JNM/(C_{60} -JNM)₂ heterostructure (see Figure S2 for JNM, C_{60} -JNM and JNM/(C_{60} -JNM)_n, n = 1 and 3). By fitting multiple curves to a pressure-deflection equation for rectangular/square membranes,^{35,36} Young's modulus (E_{Young}) can be extracted (Figure 3h and Table S1). First, we compare the mechanical properties of pristine JNM with C_{60} -JNM. To this end, the in-plane elastic modulus (E_{2d}) has to be considered.^{37–39} It equals to E_{Young} multiplied by the thickness of the sheet. The obtained E_{2d} values for JNM (9.9±1.7 N/m) and C_{60} -JNM (11.6±1.7 N/m) are of the same magnitude, which shows that the mechanical robustness of a JNM is not diminished upon its covalent functionalization. Next, we compare the mechanical properties multilayer stacks considering the respective E_{Young} values.³⁷ E_{Young} for JNM/(C_{60} -JNM)₁, JNM/(C_{60} -JNM)₂ and JNM/(C_{60} -JNM)₃ are 7.5±1.8 GPa, 7.2±1.3 GPa and 8.7±1.5 GPa, respectively (Figure 3h). It can be clearly seen that within the measurement accuracy the Young's moduli of the JNM/(C_{60} -JNM)_n (n = 1, 2 and 3) heterostructures have similar values demonstrating that the

mechanical properties are not degraded upon the assembly of the hybrid JNMs into stacks.

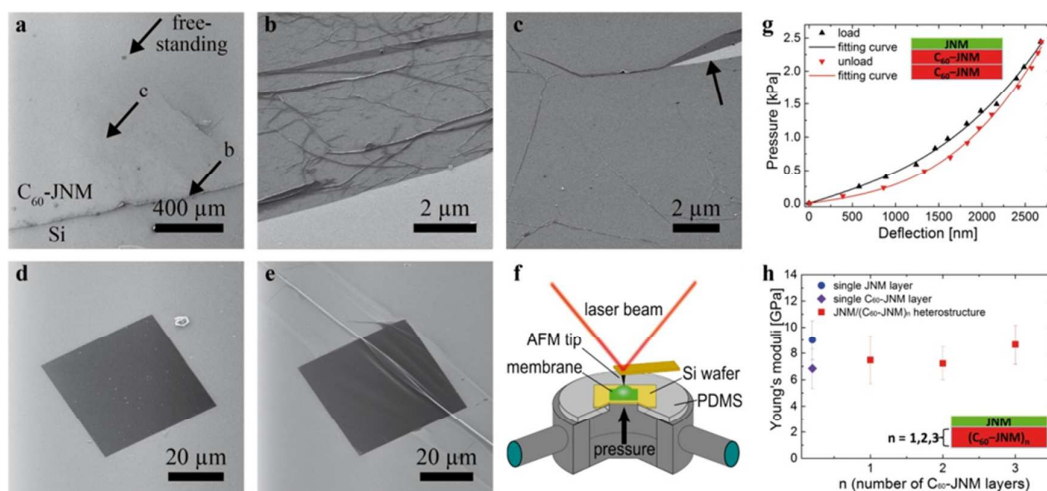


Figure 3. Helium ion microscopy (HIM) imaging of C_{60} -JNM heterostructures and their mechanical properties. a) HIM image of a C_{60} -JNM on a Si substrate with orifices. An orifice with dimensions $40 \times 44 \mu\text{m}^2$ is marked here as “free-standing”. b) Magnified HIM image of the C_{60} -JNM boundary; the corresponding place is marked in (a) with an arrow. c) Magnified HIM image of the central part of the C_{60} -JNM; the corresponding place is marked in (a) with an arrow. In (d) and (e) HIM images of an JNM-(C_{60} -JNM)₃ heterostructure spanning a Si window are shown. In (d) the nanomembrane is homogeneous whereas in (e) a fold can be recognized. f) A schematic diagram of the bulge test set-up. g) Typical pressure-deflection curves for a JNM-(C_{60} -JNM)₂ heterostructure. h) Young's moduli of JNM, C_{60} -JNM and JNM-(C_{60} -JNM)_n ($n = 1, 2$, and 3).

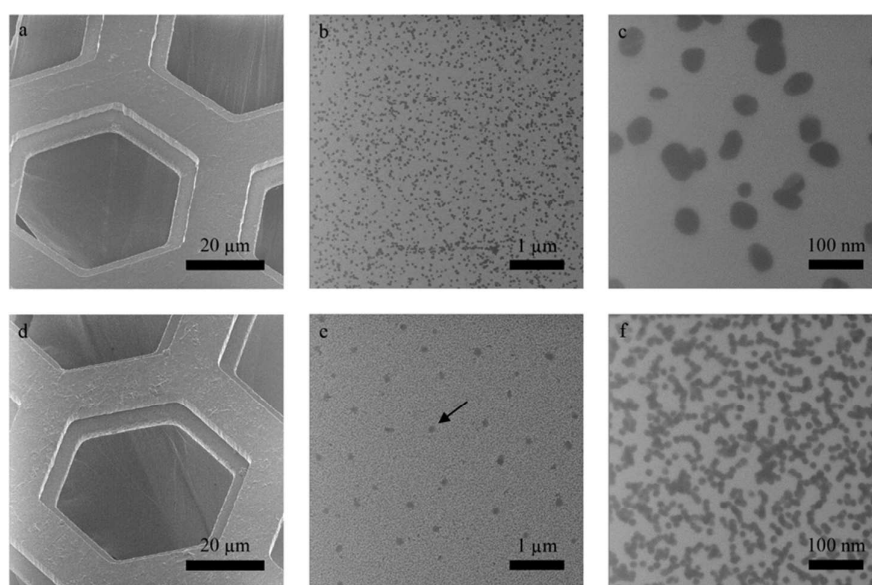


Figure 4. JNMs functionalized with Au nanoparticles on the S-face. Helium ion microscope images acquired in the secondary electron (SE) mode and scanning transmission ion modes (STIM). a) SE image of JNMs functionalized with 55 nm Au nanoparticles and transferred onto a grid. b) and c) STIM images show that the nanoparticles are uniformly distributed with an average coverage of $\sim 15\%$. d) SE image of JNMs functionalized with 16 nm Au nanoparticles and transferred onto a grid. e) and f) STIM images showing that the nanoparticles are uniformly distributed with a coverage of $\sim 50\%$. Dark areas (see the arrow in Figure e) are residues from sample preparation.

To show that for the assembly of hybrid heterostructures also the S-side of JNMs can be employed, we studied its functionalization with Au NPs (Figure 1c, Figure 4). Negatively charged Au NPs with sizes

of ~ 55 and 16 nm were used to this end. As the S-side of a JNM due to the presence of sulfonic groups is also negatively charged, a positively charged adhesive polyelectrolyte layer of

poly(diallyldimethylammonium chloride) was added to immobilize the negatively charged Au NPs. We employed scanning transmission ion microscopy (STIM) to image the hybrid nanomembranes suspending hexagonal grids (~25 μm) with the functionalized S-side oriented upwards. From statistical analysis we estimate the average coverage of the 55 and 16 nm-sized Au NPs on JNMs to be ~15% and ~50%, respectively, showing that the coverage correlates with the NP size. As a wide variety of materials can be immobilized by electrostatic interactions,² this strategy provides a flexible route to incorporate different materials into JNM-based hybrids. The modification of the S-side of JNMs with above-described method needs PMMA as a protection layer, which restricts the modification to conditions compatible with this layer. In case such a layer cannot be employed, the JNM can also be flipped over and transferred onto a new solid substrate where the originally bottom S-side becomes to be the terminal one (Figure S3-5).

Conclusions

In summary, we have presented a modular and highly applicable approach for the assembly of cm²-sized vdW hybrid heterostructures. This approach is based on the utilization of ~1 nm thick bifacial and mechanically stable JNMs, their chemical functionalization and subsequent stacking into layered heterostructures. In the present study the heterostructures of JNMs with C₆₀ and gold nanoparticles were investigated. The possibility of bifacial chemical functionalization of JNMs paves the way to hybrid vdW heterostructures with a variety of other 0D and 1D materials.

Acknowledgements

This work was supported by the Deutsche Forschungsgemeinschaft (SPP "Graphene" and Heisenberg Programme), the Volkswagenstiftung and the Alexander von Humboldt Foundation (Sofja Kovalevskaja Award to MCL). Z. Z. and X. Z. contributed equally to this work. We thank Prof. Xinliang Feng (TU Dresden) for fruitful discussions.

Notes and references

- 1 K. B. Blodgett, *J. Am. Chem. Soc.* **1934**, *56*, 495.
- 2 G. Decher, *Science* **1997**, *277*, 1232.
- 3 K. Ariga, J. P. Hill, Q. Ji, *Phys. Chem. Chem. Phys.* **2007**, *9*, 2319.
- 4 S. Srivastava, N. A. Kotov, *Acc. Chem. Res.* **2008**, *41*, 1831.
- 5 Z. Tang, Y. L. Wang, P. Podsiadlo, N. A. Kotov, *Adv. Mater.* **2006**, *18*, 3203.
- 6 J. Sagiv, *J. Am. Chem. Soc.* **1980**, *102*, 92.
- 7 J. C. Love, L. A. Estroff, J. K. Kriebel, R. G. Nuzzo, G. M. Whitesides, *Chem. Rev.* **2005**, *105*, 1103.
- 8 A. Ulman, *Introduction to Ultrathin Organic Films*, Academic, San Diego, CA **1991**.
- 9 A. K. Geim, I. V. Grigorieva, *Nature* **2013**, *499*, 419.
- 10 K. S. Novoselov, D. Jiang, F. Schedin, T. J. Booth, V. V. Khotkevich, S. V. Morozov, A. K. Geim, *Proc. Natl. Acad. Sci. U. S. A.* **2005**, *102*, 10451.
- 11 J. Sakamoto, J. van Heijst, O. Lukin, A. D. Schlüter, *Angew. Chem. Int. Ed.* **2009**, *48*, 1030.
- 12 W. Eck, A. Küller, M. Grunze, B. Völkel, A. Götzhäuser, *Adv. Mater.* **2005**, *17*, 2583.
- 13 a) M. Woszczyzna, A. Winter, M. Grothe, A. Willunat, S. Wundrack, R. Stosch, T. Weimann, F. Ahlers, A. Turchanin, *Adv. Mater.* **2014**, *26*, 4831; b) C. T. Nottbohm, A. Turchanin, A. Beyer, R. Stosch, A. Götzhäuser, *Small* **2011**, *7*, 874.
- 14 a) H. Yin, S. Zhao, K. Zhao, A. Muqsit, H. Tang, L. Chang, H. Zhao, Y. Gao, Z. Tang, *Nat. Commun.* **2015**, *6*, 6430; b) H. Tang, J. Wang, H. Yin, H. Zhao, D. Wang, Z. Tang, *Adv. Mater.* **2015**, *27*, 1117; c) H. Yin, S. Zhao, J. Wan, H. Tang, L. Chang, L. He, H. Zhao, Y. Gao, Z. Tang, *Adv. Mater.* **2013**, *25*, 6270.
- 15 T. Georgiou, R. Jalil, B. D. Belle, L. Britnell, R. V. Gorbachev, S. V. Morozov, Y.-J. Kim, A. Gholinia, S. J. Haigh, O. Makarovskiy, L. Eaves, L. A. Ponomarenko, A. K. Geim, K. S. Novoselov, A. Mishchenko, *Nature Nanotechnol.* **2013**, *8*, 100.
- 16 V. Georgakilas, M. Otyepka, A. B. Bourlino, V. Chandra, N. Kim, K. C. Kemp, P. Hobza, R. Zboril, K. S. Kim, *Chem. Rev.* **2012**, *112*, 6156.
- 17 D. Voiry, A. Goswami, R. Kappera, C. C. C. Silva, D. Kaplan, T. Fujita, M. Chen, T. Asefa, M. Chhowalla, *Nature Chem.* **2015**, *7*, 45.
- 18 S. Jiang, S. Butler, E. Bianco, O. D. Restrepo, W. Windl, J. E. Goldberger, *Nature Commun.* **2014**, *5*, 1.
- 19 H. Y. Mao, Y. H. Lu, J. D. Lin, S. Zhong, A. T. S. Wee, W. Chen, *Prog. Surf. Sci.* **2013**, *88*, 132.
- 20 J. Du, S. Pei, L. Ma, H.-M. Cheng, *Adv. Mater.* **2014**, *26*, 1958.
- 21 Z. Zheng, C. T. Nottbohm, A. Turchanin, H. Muzik, A. Beyer, M. Heilemann, M. Sauer, A. Götzhäuser, *Angew. Chem. Int. Ed.* **2010**, *49*, 8493.
- 22 W. Eck, V. Stadler, W. Geyer, M. Zharnikov, A. Götzhäuser, M. Grunze, *Adv. Mater.* **2000**, *12*, 805.
- 23 A. Turchanin, A. Götzhäuser, *Prog. Surf. Sci.* **2012**, *87*, 108.
- 24 A. Turchanin, A. Beyer, C. T. Nottbohm, X. Zhang, R. Stosch, A. S. Sologubenko, J. Mayer, P. Hinze, T. Weimann, A. Götzhäuser, *Adv. Mater.* **2009**, *21*, 1233.
- 25 A. Turchanin, D. Käfer, M. El-Desawy, C. Wöll, G. Witte, A. Götzhäuser, *Langmuir* **2009**, *25*, 7342.
- 26 M. Schnietz, A. Turchanin, C. T. Nottbohm, A. Beyer, H. H. Solak, P. Hinze, T. Weimann, A. Götzhäuser, *Small* **2009**, *5*, 2651.
- 27 P. J. Moriarty, *Surf. Sci. Rep.* **2010**, *65*, 175.
- 28 K. M. Chen, W. B. Caldwell, C. A. Mirkin, *J. Am. Chem. Soc.* **1993**, *115*, 1193.
- 29 W. B. Caldwell, K. Chen, C. A. Mirkin, S. J. Babinec, *Langmuir* **1993**, *9*, 1945.
- 30 A. Pirkle, J. Chan, A. Venugopal, D. Hinojos, C. W. Magnuson, S. McDonnell, L. Colombo, E. M. Vogel, R. S. Ruoff, R. M. Wallace, *Appl. Phys. Lett.* **2011**, *99*, 122108.
- 31 A. P. Terzyk, *Coll. Surf. A* **2001**, *177*, 23.
- 32 S. Heid, F. Effenberger, K. Bierbaum, M. Grunze, *Langmuir* **1996**, *12*, 2118.
- 33 N. Tillman, A. Ulman, T. L. Penner, *Langmuir* **1989**, *5*, 101.
- 34 H. Sugimura, H. Yonezawa, S. Asai, Q. W. Sun, T. Ichii, K. H. Lee, K. Murase, K. Noda, K. Matsushige, *Coll. Surf. A* **2008**, *321*, 249.
- 35 X. H. Zhang, A. Beyer, A. Götzhäuser, *Beilstein J. Nanotechnol.* **2011**, *2*, 826.
- 36 X. H. Zhang, C. Neumann, P. Angelova, A. Beyer, A. Götzhäuser, *Langmuir* **2014**, *30*, 8221.
- 37 C. Lee, X. Wie, J. W. Kysar, J. Hone, *Science* **2008**, *521*, 385.
- 38 Z. Zheng, C. S. Ruiz-Vargas, T. Bauer, A. Rossi, P. Payamyar, F. Schiffmann, J. VandeVondele, A. Stemmer, J. Sakamoto, A. D. Schlüter, *Macromol. Rapid Commun.* **2013**, *34*, 1670.
- 39 Z. Zheng, L. Opilik, F. Schiffmann, W. Liu, G. Bergamini, P. Ceroni, L. Lee, A. Schütz, J. Sakamoto, R. Zenobi, J. VandeVondele, A. D. Schlüter, *J. Am. Chem. Soc.* **2014**, *136*, 6103.
- 40 G. Frens, *Nature* **1973**, *241*, 20.



Nanoscale

COMMUNICATION

Nanoscale Accepted Manuscript